Solution Structures of a Highly Insecticidal Recombinant Scorpion α-Toxin and a Mutant with Increased Activity[†,‡]

Vitali Tugarinov,[§] Irina Kustanovich,[§,||] Noam Zilberberg,[⊥] Michael Gurevitz,[⊥] and Jacob Anglister*[,§]

Department of Structural Biology, The Weizmann Institute of Science, Rehovot 76100, Israel, and Department of Botany, Faculty of Life Sciences, Tel-Aviv University, Ramat Aviv 69978, Tel-Aviv, Israel

Received June 21, 1996; Revised Manuscript Received December 23, 1996[⊗]

ABSTRACT: The solution structure of a recombinant active α-neurotoxin from *Leiurus quinquestriatus hebraeus*, LqhαIT, was determined by proton two-dimensional nuclear magnetic resonance spectroscopy (2D NMR). This toxin is the most insecticidal among scorpion α-neurotoxins and, therefore, serves as a model for clarifying the structural basis for their biological activity and selective toxicity**.** A set of 29 structures was generated without constraint violations exceeding 0.4 Å. These structures had root mean square deviations of 0.49 and 1.00 Å with respect to the average structure for backbone atoms and all heavy atoms, respectively. Similarly to other scorpion toxins, the structure of LqhαIT consists of an α-helix, a three-strand antiparallel β-sheet, three type I tight turns, a five-residue turn, and a hydrophobic patch that includes tyrosine and tryptophan rings in a "herringbone" arrangement. Positive ϕ angles were found for Ala^{50} and Asn^{11}, suggesting their proximity to functionally important regions of the molecule. The sample exhibited conformational heterogeneity over a wide range of experimental conditions, and two conformations were observed for the majority of protein residues. The ratio between these conformations was temperature-dependent, and the rate of their interconversions was estimated to be on the order of $1-5\ s^{-1}$ at 308 K. The conformation of the polypeptide backbone of LqhαIT is very similar to that of the most active antimammalian scorpion α-toxin, AaHII, from *Androctonus australis* Hector (60% amino acid sequence homology). Yet, several important differences were observed at the 5-residue turn comprising residues Lys^{8}-Cys^{12}, the C-terminal segment, and the mutual disposition of these two regions. 2D NMR studies of the R64H mutant, which is 3 times more toxic than the unmodified LqhαIT, demonstrated the importance of the spatial orientation of the last residue side chain for toxicity of LqhαIT.

Scorpion α-neurotoxins bind with high affinity to voltage-dependent sodium channels of neuronal membranes (Catterall, 1977; Beneski & Catterall, 1980) and affect their gating properties. These toxins reveal structural similarity and high sequence homology (Rochat et al., 1979; Dufton & Rochat, 1984) but display varying degrees of selectivity toward insect and mammalian sodium channels (Gordon et al., 1996).

Despite the fact that several three-dimensional structures of long-chain scorpion toxins have been determined (Pashkov et al., 1988; Darbon et al., 1991; Lebreton et al., 1994; Landon et al., 1996; Jablonsky et al., 1995; Fontecilla-Camps et al., 1988; Zhao et al., 1992), the location of the toxic site of these neurotoxins and the molecular basis for their biological activity and phylogenetic selectivity remain unknown. All long-chain scorpion neurotoxins have regions of high sequence homology and similar secondary and tertiary structures: they contain an α-helix of approximately 2.5 turns, a three-strand antiparallel β-sheet, several tight turns, four highly conserved disulfide bridges, and a hydrophobic patch made of the side chains of several aromatic and nonpolar residues. It has been suggested (Fontecilla-Camps, 1989; Darbon et al., 1991) that the hydrophobic patch is a conserved part of all scorpion toxins governing the interactions of these polypeptides with their receptors, whereas the adjacent regions are variable and may modulate their selectivity to insects or mammals. Elucidation of the molecular basis for this specificity may be achieved via genetic modifications and comparative structural analyses.

LqhαIT,[1] a 64-residue toxin from *Leiurus quinquestriatus hebraeus* venom, was classified as an α-toxin on the basis of its structural and functional similarities to other scorpion

[†] This work was supported by grants from the U.S.−Israel Binational Science Foundation (Grant 95-246 to J.A.), the U.S.−Israel Binational Agricultural Research and Development (BARD) (Grant IS-2486-94C to M.G.), and the Israeli Ministry of Agriculture (Grant 891-0112-95 to M.G.).

[‡] The coordinates of LqhαIT were deposited with the Brookhaven Protein Data Bank under the ID codes 1LQH (for 29 NMR models) and 1LQI (for minimized average structure).

* Address correspondence to this author.

[§] The Weizmann Institute of Science.

[||] Present address: Department of Biological Chemistry, Institute of Life Sciences, The Hebrew University, Givat-Ram, Jerusalem 91904, Israel.

[⊥] Tel-Aviv University.

[⊗] Abstract published in *Advance ACS Abstracts,* February 15, 1997.

[1] Abbreviations: LqhαIT, *Leiurus quinquestriatus hebraeus* α-insect toxin; Lqq4, *Leiurus quinquestriatus quinquestriatus* 4 scorpion toxin; LqqIII, *Leiurus quinquestriatus quinquestriatus* III scorpion toxin; BeM_9, *Buthus eupeus* M_9 scorpion toxin; AaHII, *Androctonus australis* Hector II toxin; BPTI, bovine pancreatic trypsin inhibitor; NMR, nuclear magnetic resonance spectroscopy; NOE, nuclear Overhauser effect; NOESY, two-dimensional nuclear Overhauser enhancement spectroscopy; HOHAHA, two-dimensional homonuclear Hartmann−Hahn spectroscopy; PH-COSY, two-dimensional phase-sensitive correlation spectroscopy; DQF-COSY, two-dimensional double-quantum filtered correlation spectroscopy; TPPI, time-proportional phase incrementation; CHS, conserved hydrophobic surface; rmsd, root mean square deviation; HPLC, high-performance liquid chromatography; PCR, polymerase chain reaction; 2D and 3D, two- and three-dimensional, respectively.

S0006-2960(96)01497-3 CCC: $14.00

α-toxins (Eitan et al., 1990). It slows the inactivation process of insect sodium channels, and its binding to the receptor site on neuronal membranes is competitively inhibited by the sea anemone toxin ATXII and enhanced by veratridine (Gordon & Zlotkin, 1993). Radiolabeled LqhαIT binds to a single class of high-affinity sites on insect neuronal membranes with $K_d = 0.2$ nM and 0.02 nM in locust and cockroach, respectively, and practically does not displace AaHII from its receptor site on rat brain synaptosomes (Gordon et al., 1996). LqhαIT is toxic to mice at relatively high concentrations, as opposed to other scorpion α-toxins like AaHII (Zilberberg et al., 1996; Gordon et al., 1996), and appears to recognize an α-toxin binding site on both insect and mammalian sodium channels. The uniqueness of LqhαIT is manifested by its apparent higher affinity for insect versus mammalian channels (Gordon et al., 1996). This toxin thus serves as a suitable model for understanding the structural basis for toxicity and phylogenetic selectivity of α-neurotoxins (Zilberberg et al., 1996).

Herein we report the detailed NMR solution structures of the most insecticidal recombinant scorpion α-toxin, LqhαIT, and a mutant, R64H, exhibiting 3-fold increased activity. Our data suggest an important role for those residues in LqhαIT which differ from LqIII toxin (Landon et al., 1996) and shed light on the contribution of the C-terminal residue to the biological activity of LqhαIT. These NMR results are compared with the X-ray structure of the most potent antimammalian α-toxin, AaHII (Fontecilla-Camps et al., 1988), with the NMR structure of a highly homologous toxin, LqqIII (Landon et al., 1996), and with Lqq4 (Kopeyan et al., 1985). The structural differences between these α-neurotoxins may account for their different animal group specificities and other aspects of biological activity.

MATERIALS AND METHODS

Sample Preparation. Functional LqhαIT toxin was produced using a recently developed efficient bacterial expression system (Zilberberg et al., 1996). The recombinant toxin was purified to 99% by reverse-phase HPLC on a C_{18} column as described elsewhere (Zilberberg et al., 1996). Mass-spectral analysis of the recombinant LqhαIT was performed by matrix-assisted laser desorption time-of-flight method and showed a single peak corresponding to the molecular mass of the toxin. A 2.0 mM solution of the toxin containing 10 mM sodium phosphate buffer and 0.05% sodium azide was prepared in 90% H_2O/10% D_2O. Another sample was prepared in 99.99% D_2O by two cycles of redissolving lyophilized toxin in 99.8% D_2O, incubation for 24 h at 37 °C, lyophilization, and final redissolving in 99.99% D_2O. The sample in D_2O contained 10 mM sodium phosphate buffer.

The R64H mutant of LqhαIT was generated via PCR, and the toxin was produced as previously described (Zilberberg et al., 1996). The NMR sample of the mutant was prepared in 90% H_2O/10% D_2O identically to the sample of the unmodified toxin.

NMR Measurements. 2D ^{1}H NMR experiments were recorded on a Bruker AM500 spectrometer in the phase-sensitive mode using the TPPI method (Marion & Wüthrich, 1983). The carrier frequency was set on the HDO resonance. Water suppression was achieved by presaturation during a relaxation delay of 1.3 s in the HOHAHA and PH-COSY experiments and 1.5 s in the NOESY experiments. HOHAHA spectra (Davis & Bax, 1985) were obtained using the WALTZ (Shaka et al., 1983) pulse sequence with several mixing periods ranging from 30 to 120 ms. The NOESY experiments (Kumar et al., 1980; Macura & Ernst, 1981) were recorded at three mixing times: 80, 150, and 200 ms. DQF-COSY (Piantini et al., 1982; Braun et al., 1981) and PH-COSY (Marion & Wüthrich, 1983) spectra were obtained by conventional procedures. All experiments were recorded with a spectral width of 7040 Hz and with 4K or 8K data points in F_2 and 512 increments in F_1 dimension. Spectra were processed with UXNMR software (Bruker Analytische Messtechnik GmbH) on an Iris 4D/35 workstation. The first serial experiment and the first point in each serial row of all spectra were half-weighted in order to reduce t_2 ridges. A zero-filling in the F_2 dimension and a square sine bell window function shifted by 60° were applied prior to two-dimensional Fourier transformation. The spectra recorded in H_2O were baseline-corrected in the F_2 dimension with quadratic polynomial function to reduce water peak lobes.

NMR spectra of the 90% H_2O/10% D_2O solution were recorded at pH 4.8 and 5.8 at 308 K and at pH 5.8 at 320 K. Some spectra were obtained also at 295 K and 303 K but exhibited much poorer signal-to-noise ratios. NOESY and HOHAHA spectra at pH 3.0 and 308 K were recorded as well.

To identify slowly exchanging amide protons, the toxin was lyophilized from H_2O and redissolved in 99.8% D_2O at pH 4.8. The acquisition of the HOHAHA spectrum started 3 h later and continued for 10 h. Amide protons still giving rise to cross peaks were considered to be in slow exchange with the solvent.

To analyze the temperature dependence of the population of the two conformational forms of LqhαIT, several short (256 real points in F_1 dimension) HOHAHA data sets were acquired at 295, 300, 310, 320, and 325 K at pH 4.8.

$^3J_{HNH\alpha}$ coupling constants were measured from HOHAHA spectra acquired with 8K data points in the F_2 dimension and subsequently zero-filled to 16K (Driscoll et al., 1989). The in-phase doublets were fitted to Lorentzian line shapes, and $^3J_{HNH\alpha}$ were derived only from the doublets with a reasonably good fit. $^3J_{H\alpha H\beta}$ couplings, used in stereospecific assignments, were obtained from PH-COSY spectra, measured in D_2O with 8K data points in the F_2 dimension and subsequent zero-filling to 16K. DQF-COSY spectra exhibited rather poor signal-to-noise ratios for both $^3J_{HNH\alpha}$ and $^3J_{H\alpha H\beta}$ measurements.

HOHAHA and NOESY spectra of the R64H mutant in H_2O were recorded on a Bruker DMX600 spectrometer at 308 K and pH 4.8 and processed on SGI Indy workstation with the XWINNMR software (Bruker Analytische Messtechnik GmbH). The HOHAHA spectrum was recorded with a mixing time of 70 ms using WALTZ pulse sequence for isotropic mixing, whereas the NOESY spectrum was collected with a 200-ms mixing time. Efficient water suppression was achieved by WATERGATE (WATER suppression by GrAdient-Tailored Excitation) pulse sequence (Piotto et al., 1992). The duration of the gradient pulses was 3 ms. Both spectra were processed in the same way as those of the unmodified toxin, thus allowing their direct comparison using AURELIA software package (Neidig et al., 1995).

NOE Measurements and Experimental Restraints. Structure determination by NMR is based on a large number of

restraints on proton−proton distances that are obtained from the analyses of the NOESY spectrum of the protein (Wüthrich, 1986, 1989). The NOE build-up curves obtained from NOESY spectra recorded with 80, 150, and 200-ms mixing times, showed no signs of spin diffusion for the NOESY spectra recorded with a 200-ms mixing period. Thus, it was concluded that the 200-ms data may be used for structure derivation at the level of approximation usual for NMR studies (peaks classified as weak, medium, and strong). The calibration curve for distance restraints was based on the volume integrals of sequential $H^{\alpha}(i)/H^{N}(i+1)$ cross peaks of the residues involved in the β-sheet. The distance between these protons is known to be 2.2 Å. In the aromatic and H^{N}/H^{N} regions of the spectrum, the volumes of sequential $H^{N}(i)/H^{N}(i+1)$ peaks of α-helical residues with a known distance of 2.8 Å were chosen as a reference. And finally, the H^{α}/H^{α} interstrand cross peaks of the β-sheet (corresponding to 2.3 Å) were used as a reference for the NOE contacts in the aliphatic region of the spectrum, recorded in D_2O. The NOEs were divided into three classes with upper limit distances of 2.7, 3.3, and 5.0 Å. The lower bound distance was 1.8 Å in all cases. The long- and medium-range restraints involving side-chain protons were further relaxed by an additional 0.5 Å to account for internal motions and proton multiplicity. Pseudoatom corrections were applied where necessary at initial stages of the structure calculations (Wüthrich et al., 1983), whereas final structures were generated using $\langle r^{-6} \rangle$ averaging of distance restraints (Brünger et al., 1986; Nilges, 1993) for unresolved and stereospecifically unassigned NOE interactions.

For each of the four disulfide bridges, i.e., Cys^{12}/Cys^{63}, Cys^{16}/Cys^{36}, Cys^{22}/Cys^{46}, and Cys^{26}/Cys^{48}, three constraints were given in the input list: $d_{S\gamma-S\gamma}$ was constrained between 1.9 and 2.1 Å and cross-bridge $d_{S\gamma-C\beta}$ was constrained between 2.9 and 3.1 Å. Two constraints were applied for each hydrogen bond: the H···O distance was constrained between 1.5 and 2.3 Å, and the corresponding N···O distance between 2.5 and 3.3 Å.

Stereospecific assignments were based on a combined use of $^{3}J_{H\alpha H\beta}$ couplings and NOE information from H^{α}/H^{β} and H^{N}/H^{β} cross peaks (Zuiderweg et al., 1985; Wagner et al., 1987; Basus, 1989). The intensities of H^{α}/H^{β} and H^{N}/H^{β} peaks were measured from NOESY spectra recorded with a 80-ms mixing time. For stereospecific assignments of valine methyls as well as the χ_1 angle determination for threonine and isoleucine, the intensities of $H^{\alpha}/C^{\gamma}H_3$ and $H^{N}/C^{\gamma}H_3$ were also used. The χ_1 angles were constrained to $+60°(\pm 60°)$, $-60°(\pm 60°)$, or $180°(\pm 60°)$.

Structure Calculations. Structure calculations were performed on Sun Sparc 10 and Silicon Graphics 4D/35 workstations with the program XPLOR/dg version 3.1 (Brünger, 1992). The structures were displayed for analysis on a Silicon Graphics workstation using the InsightII (MSI Technologies, Inc.) and MOLMOL (Spectrospin AG) programs.

The hybrid distance geometry−dynamical simulated annealing method (Nilges et al., 1988) was used for structure generation with the XPLOR 3.1 program (Brünger, 1992). The structure calculation was accomplished in several steps. Initial input list of distance and torsional constraints did not include the data from stereospecific assignments and χ_1 angle restraints. It included only a limited number of hydrogen bonds that were unambiguously identified at the initial stage. The substructures, generated by metric matrix distance geometry algorithm, were extended to C^{δ} and C^{ϵ} atoms, as there were numerous NOE contacts involving the side chains of aromatic residues. The NOE force constant was set to 50 kcal/mol for all calculations. After two rounds of simulated annealing refinement with 2000 cooling steps from 1000 to 100 K, initial low-resolution structures were obtained. These were used to complete assignments of ambiguous NOE peaks, deduce possible oxygen acceptors for slowly exchanging labile hydrogens, and confirm a number of stereospecific assignments in cases of ambiguities.

The structure calculations for the R64H mutant of LqhαIT were performed on the basis of the final coordinates of the unmodified LqhαIT. Intra- and interresidual constraints were introduced for His^{64}, and the peaks of the residues which exhibited changes in chemical shifts (see Results) were reintegrated. All other peaks in the NOESY spectrum did not exhibit any significant changes in volume integral values after calibration. Several rounds of simulated annealing refinements were performed with 4000 cooling steps from 2000 to 100 K till all new constraints were satisfied to 0.4 Å.

RESULTS

Sequential Assignment of Resonances. The spin systems were identified using DQF-COSY and HOHAHA spectra recorded with various mixing times in H_2O and in D_2O at pH 4.8 and 5.8 at 308 K as well as the spectrum recorded at pH 5.8 at 320 K. The information obtained from these experiments was supplemented by the analyses of NOESY spectra, recorded in H_2O and D_2O at 200-ms mixing time. The $C^{\alpha}H$ and $C^{\beta}H$ resonances of tyrosine, tryptophan, and phenylalanine were tentatively assigned by the presence of $C^{\delta}H$ to $C^{\beta}H$ and $C^{\delta}H$ to $C^{\alpha}H$ NOE cross peaks in both D_2O and H_2O spectra. Likewise, seven asparagines and one glutamine residue were tentatively identified by $N^{\delta}H$ to $C^{\beta}H$ (asparagine) and $N^{\epsilon}H$ to $C^{\gamma}H$ (glutamine) intraresidual cross peaks, appearing only in H_2O spectra. The identification of all four arginine residues was aided by cross peaks from $N^{\epsilon}H$ to all side-chain protons in HOHAHA spectra recorded at pH 4.8. Final amino acid type identification for the majority of spin systems was achieved at the stage of sequence-specific assignments.

The procedure developed by Wüthrich and his co-workers (Wüthrich, 1986) was applied for sequential resonance assignments using NOESY spectra recorded with a 200-ms mixing time. The stretches of possible amino acid types were matched to locations in the protein on the basis of the known primary sequence (Figure 1). Sequential NOE connectivities $H^{\alpha}(i)/H^{N}(i+1)$ and/or $H^{N}(i)/H^{N}(i+1)$ were found for all residues of the protein, except Lys^{41}/Tyr^{42}, Asn^{9}/Tyr^{10}, and prolines. For prolines, the $H^{\alpha}(i)/H^{\delta}(i+1)$ connectivities observed in D_2O spectra were used. These peaks were rather strong for all three prolines of the protein, indicating that all prolines were in the *trans* configuration. No sequential NOE cross peaks were found between H^{N} of Tyr^{42} and H^{α} of Lys^{41} because of the chemical shift degeneracy of amide protons at lower temperatures and pH values and presumably fast exchange of Lys^{41} H^{N} with the solvent at higher temperatures and pH values. The spin system of Asn^{9} could not be unambiguously assigned from fingerprint regions of either DQF-COSY or HOHAHA spectra. The chemical

```
          0    5    10   15   20   25   30   35   40   45   50   55   60
LqhaIT    MVRDAYIAKNYNCVYECFR··DAYCNELCTKNGASSGYCQWAGKYGNACWCYALPDNVPIRVPGKCR
AaHII      -K-G--VDDV--T-F-G-··N-----E---LKGE-------SP-----Y--K---H-RTKG--R-H
LqqIII     ------------------··-S---D-----------------------------------H
Lqq4      G-------DDK----T-GS··NS---TE---D--E------L---------IK---K----I-----
BeM9       A------KPHD-----YNPKGS---D---E---E-----IL---------IQ--------I----H
```

FIGURE 1: Aligned amino acid sequences of LqhαIT and homologous scorpion α-neurotoxins. For AaHII, LqqIII, Lqq4, and BeM_9 only the residues different from LqhαIT are shown. Dots correspond to the deletion necessary to align the sequences with BeM_9. Sequence numbering of LqhαIT does not include the first methionine (number 0) to make it consistent with the sequence numbering of homologous proteins. This methionine was added to the sequence to enable bacterial expression.

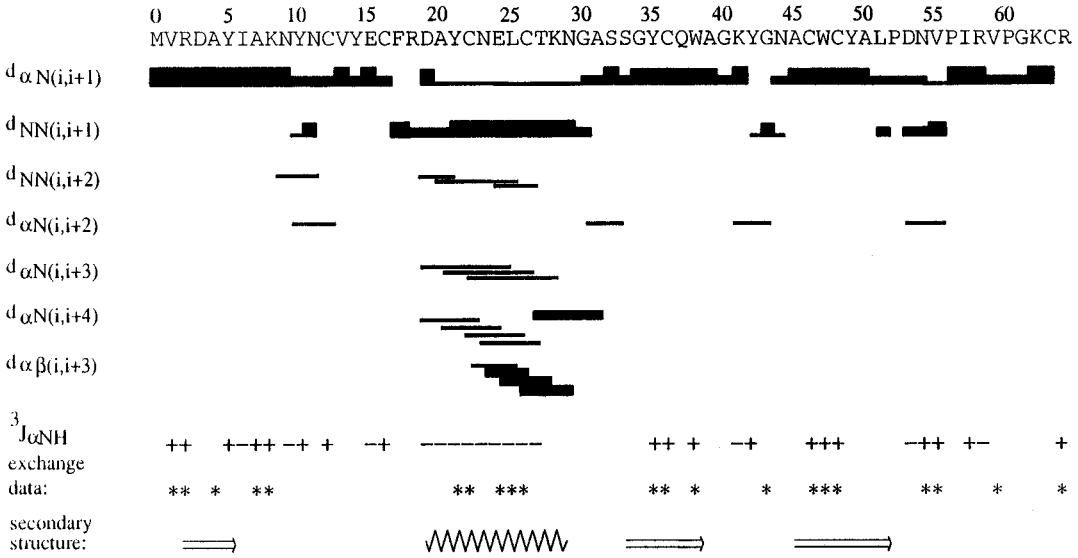

FIGURE 2: Amino acid sequence of LqhαIT and a summary of the NOE connectivities used in the sequential assignment procedure and the structure determination. The data were obtained from a NOESY spectrum recorded at 308 K and pH 4.8 with a 200-ms mixing time. For prolines, sequential NOEs involving $C^{\delta}H$ instead of H^N are indicated. The asterisks indicate slowly exchanging amide protons. $^3J_{HNH\alpha}$ coupling constants greater than 7 Hz are represented with plus signs, while minus signs correspond to coupling constants less than 6 Hz. The locations of the secondary structure elements found in LqhαIT are also indicated. Sequence numbering of LqhαIT excludes the first methionine, engineered for the bacterial expression, to make it consistent with the sequence numbering of homologous proteins.

shifts of its resonances were subsequently deduced from the analyses of the aliphatic regions of the spectra and its numerous intraresidual NOE contacts. The summary of sequential and medium-range NOE contacts as well as amide proton exchange data and $^3J_{HNH\alpha}$ coupling constants are presented in Figure 2. Several bleached-out or overlapping HOHAHA peaks were assigned from the spectrum recorded at pH 5.8 and 320 K. Likewise, the $H^{\alpha}(i)/H^N(i+1)$ NOE connectivities: Arg^2/Asp^3, Glu^{15}/Cys^{16}, and Tyr^{42}/Gly^{43}, totally bleached out by water presaturation at pH 4.8, were established from the spectrum obtained at pH 5.8 and 320 K.

Identification of Secondary Structure Elements of LqhαIT. The determination of the secondary structure of the toxin was based on the unique NOE cross peaks, coupling constants, and slow amide protons exchange rate characteristic of different secondary structure elements (Wüthrich, 1986). For example, α-helices are characterized by the coexistence of strong $H^N(i)/H^N(i+1)$ and medium $H^{\alpha}(i)/H^N(i+1)$ connectivities, as well as small (<5 Hz) $^3J_{HNH\alpha}$ couplings. On the other hand, β-sheets are characterized by strong $H^{\alpha}(i)/H^N(i+1)$ connectivities, by the absence of the connectivities typical of α-helices, and by large (>7 Hz) $^3J_{HNH\alpha}$ couplings. A regular 2.8-turn α-helix was observed for residues $Asp^{19}-Lys^{28}$ (Figure 2), and a three-stranded antiparallel β-sheet (residues 2−5, 33−38, and 44−51) was inferred from long-range backbone−backbone interactions and slow exchange of the amide protons. Numerous side chain−side chain and backbone−side chain NOE interactions were also observed between the first and third and between the first and fourth residues of the α-helix and between close residues across the strands of the β-sheet.

Tight turns are characterized by two medium-to-strong consecutive $H^N(i)/H^N(i+1)$ interactions, accompanied by weak $H^{\alpha}(i)/H^N(i+2)$ NOEs and characteristic patterns of *J*-couplings for each type of turn (Wüthrich, 1986). Two regular tight turns ($Pro^{52}-Val^{55}$ and $Gly^{40}-Gly^{43}$) and a 5-residue turn (Lys^8-Cys^{12}) were identified by characteristic NOE patterns (Figure 2). However, the classification of tight turns is rarely possible only on the basis of NOE intensities. In our particular case, small $^3J_{HNH\alpha}$ couplings for Asp^{53} and Lys^{41} at $i+1$ positions and large $^3J_{HNH\alpha}$ couplings for Asn^{54} and Tyr^{42} at $i+2$ positions of their respective turns, allowed us to classify both $Pro^{52}-Val^{55}$ and $Gly^{40}-Gly^{43}$ turns as type I β-turn. The positioning and classification of the turn connecting the α-helix with the β-sheet (residues 29−33) was not clear from NMR data and was obtained at later stages of the structure determination.

Deviations of chemical shifts of H^{α} protons from their random coil values were suggested to be a useful indicator of secondary structure (Wishart et al., 1991, 1992). Usually, negative deviations for a number of consecutive residues are indicative of an α-helical structure, whereas positive values are typical of a β-structure. In our case, these deviations correlate very well with the helical structure (residues 19−28) and with the majority of the residues in the β-sheet (data not shown). However, strong inconsistencies were observed for Ala^4 and Ala^{50}. In the case of Ala^4, these inconsistencies

may be caused by strong ring-current shifts as evidenced by numerous NOE contacts between the ring protons of Trp^{47} and H^{α} of Ala^{4}. As for Ala^{50}, it adopts an unusual backbone conformation in the final structures of LqhαIT (see below) and disrupts the hydrogen-bonding pattern of the β-sheet. It thus constitutes a β-bulge, and its unusual conformation may be partially responsible for the upfield shift of its H^{α} resonance by 0.85 ppm relative to its random-coil value.

Other Long-Range NOEs. The characteristic hydrophobic patch that is common to scorpion toxins (Fontecilla-Camps et al., 1982, 1988; Fontecilla-Camps, 1989) was manifested by numerous NOEs between different aromatic side chains of the molecule as well as strong deviations of chemical shifts from their random-coil values. A dense network of NOE interactions included aromatic protons of Tyr^{5}, Tyr^{35}, Tyr^{42}, Trp^{47}, and Tyr^{49}.

Long-range side chain−side chain and side chain−backbone NOE contacts between already assigned cysteine residues provide strong evidence for the actual existence of four covalent S−S bonds at expected positions. These disulfide bridges are highly conserved in all known structures of scorpion toxins, except for one difference found in excitatory toxins (Fontecilla-Camps, 1989).

Numerous interactions of the C-terminal residues with the 5-residue turn formed by residues Lys^{8}−Cys^{12} were observed in the NOESY spectra. These interactions involve both the backbone and the side-chain protons of the C-terminal residue, Arg^{64}. This region of the molecule was characterized by 16 long-range NOE interactions between both Arg^{64} and Cys^{63} and the side chains of Asn^{9}, Tyr^{10}, Asn^{11}, and Cys^{12}. Also, Arg^{58} interacts with the 5-residue turn, as was manifested by many long-range NOE interactions between Asn^{11} and Cys^{12} and the side-chain protons of Arg^{58}. The NOE interactions of Arg^{58} are indicative of very similar mutual spatial arrangements of its side chain and the 5-residue turn in LqhαIT and AaHII structures.

Stereospecific Assignments and Hydrogen Bonds. Eleven pairs of resolved β-methylene protons as well as the methyls of Val^{13} and Val^{59} were stereospecifically assigned. The χ_1 angle restraints were deduced for Ile^{6}, Thr^{27}, and Ile^{57}. Nine hydrogen-bond acceptors were unambiguously identified in the secondary structure elements of the toxin on the basis of slow amide hydrogen exchange data and characteristic NOE patterns (Figure 2). These conclusions were altogether facilitated by the preliminary low-resolution structures of LqhαIT.

Structure Calculations. The calculation of 60 structures using all NOE and dihedral constraints derived from spectral data gave 32 structures without NOE violations exceeding 0.5 Å, with no torsional constraint violations exceeding 5°, and with a good covalent geometry. These structures were subjected to extensive analysis to obtain further restraints.

A number of additional stereospecific assignments were made on the basis of the calculated structures. Namely, the resolved δ-methyls of Leu^{51}, Leu^{25}, and γ-methyls of Val^{55} were assigned stereospecifically on the basis of different long-range NOEs to each of the methyls of these residues. Forty new hydrogen-bond constraints were added to the input list. These were deduced primarily from very short H···O and N···O distances in at least 80% of the calculated structures. Hydrogen bonds to the carboxylates of Asp^{3} and Asp^{19} were deduced from the structure and were supported by significant changes in chemical shifts of amide protons in the HOHAHA spectrum recorded at pH 3.0. For instance, the amide hydrogen of Ala^{50} was shifted by 0.8 ppm upfield, possibly due to protonation of the spatially adjacent carboxylate of Asp^{3} at pH 3.0.

The total number of NOE distance constraints used at the final stages of structure calculation was 1082, including 288 long-range ($|i - j| > 5$) and 153 medium-range ($1 < |i - j| \leq 5$) constraints. Seventy-two torsional angle constraints were used in the calculations. These included 51 ϕ and 21 χ_1 angle constraints.

Normally, protein structures generated by distance geometry and/or simulated annealing tend to be slightly expanded and sometimes exhibit a number of poor nonbonded contacts (Clore & Gronenborn, 1989). For simulated annealing this may be a minor artifact, caused by replacing all nonbonded interactions by a simple repulsion term. In our initial calculations, all the structures obtained after simulated annealing refinement had positive values of Lennard−Jones potential (it was not included during calculations and was measured independently with the CHARMM empirical force field). The extensive use of pseudoatoms for unresolved methyl resonances of valine and leucine and degenerate resonances of aromatic ring protons led to a significant loss of resolution as a result of more relaxed distance restraints. Furthermore, for many of the observed NOE contacts none of the protons in the structure were within NOE distance, although the distance restraints on the pseudoatoms were not violated. This was especially true for abundant NOE interactions between aromatic protons, since pseudoatom corrections in this case amount to 2 Å. In order to solve this problem and to eliminate poor nonbonded contacts, two additional cycles of simulated annealing refinement were carried out with $\langle r^{-6} \rangle$ averaging of distance restraints for unresolved and stereospecifically unassigned resonances (Brünger et al., 1986; Nilges, 1993). This last round of calculations was performed without pseudoatom corrections. The final set of 29 structures was much more consistent with the NMR data, exhibited negative Lennard−Jones potentials, and had almost the same values of total penalty function as the structures obtained using pseudoatom corrections.

The final set of 29 structures with no NOE violations exceeding 0.4 Å, no torsional constraint violations exceeding 5°, good covalent geometry, no poor nonbonded contacts, and negative values of Lennard−Jones potentials was subjected to detailed final analysis and comparisons with homologous structures. The statistical data for this final set of structures are presented in Table 1. The overall structure of the toxin is well-defined with rmsd of 0.49 and 1.00 Å for the backbone and all heavy atoms, respectively (the first methionine excluded). Figure 3 shows the best-fit superposition of the backbone structures resulting from the last cycle of simulated annealing refinement. The secondary structure is very well-defined with rmsd values of 0.33 and 0.37 Å for the backbone atoms of the α-helix and β-sheet residues, respectively. The distribution of rmsd values versus residue number is shown in Figure 4. The most poorly defined regions coincide with the Lys^{8}−Cys^{12} 5-residue turn, Gly^{40}−Gly^{43} type I turn, and four C-terminal residues. Generally, the rmsd values show inverse correlation with the number of NOE constraints (data not shown).

Conformational Heterogeneity. In addition to the cross peaks that were assigned to the main conformation of the toxin, the HOHAHA and NOESY spectra exhibited numer-

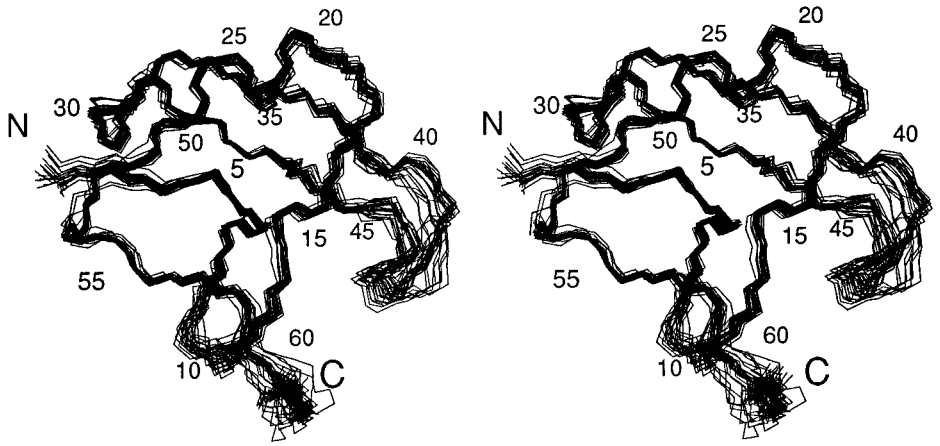

FIGURE 3: Stereo view of the best-fit superposition of 29 LqhαIT backbone structures. Each fifth residue is numbered.

Table 1: Structural Statistics for 29 LqhαIT Structures[a]

Rms Deviations from Experimental Constraints	
NOE (Å)	0.028
dihedral angles (deg)	0.460
Rms Deviations from Idealized Covalent Geometry	
bonds (Å)	0.003
angles (deg)	0.610
impropers (deg)	0.462
Energies (kcal mol^{-1})	
overall	195.3
bonds	8.881
angles	97.64
impropers	19.20
NOE	38.22
dihedral constraints	1.023
repel	30.34
vdW[b]	−116.3
Rms Deviations vs the Average Structure (Å)	
backbone atoms	0.49
side-chain atoms	1.24
all heavy atoms	1.00
backbone atoms (residues 1−60)	0.43

[a] The first methionine residue was not included in rmsd calculations. [b] Full van der Waals potential was not used in the structure calculations and was estimated afterwards with the Charmm force field.

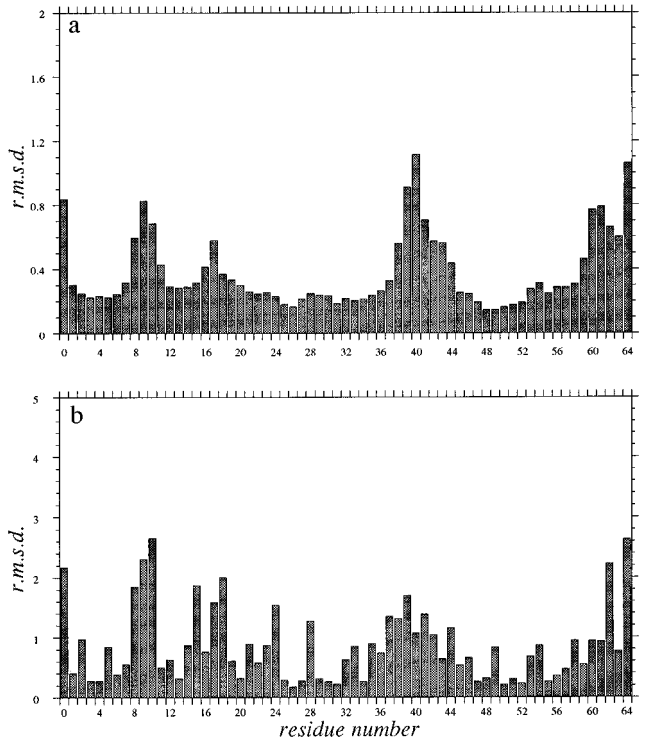

FIGURE 4: Distribution of atomic rmsd per residue with respect to the mean structure for (a) the backbone atoms and (b) all heavy atoms.

ous weaker cross peaks that caused further complication of the spectral analysis. No exchange peaks between the two forms could be observed in the NOESY spectra because of very small differences in the chemical shifts between the major and minor forms (usually not more than 0.1 ppm). The existence of any significant amount of impurities or degradation products in the sample was ruled out on the basis of mass-spectral and RP-HPLC analyses as well as SDS−polyacrylamide gel electrophoresis (data not shown). Furthermore, since the studied toxin is a recombinant one, it cannot be contaminated with other toxins. In some cases (when the differences in chemical shifts of the minor and major peaks were observable) it was possible to make sequential assignment for the minor form. The population of the minor form (evaluated from peak volume integrals at various temperatures) changed from 20% ± 3% at 300 K to 35% ± 3% at 325 K (pH 4.8). It was about 28% at 308 K and pH 5.8, which corresponds to ΔG of the major to minor form transformation of about 0.6 kcal/mol at these conditions. No changes in the population of the minor form more than ±2−3% (of the total concentration of the toxin) were observed at pH 4.8 vs pH 5.8. In the spectrum recorded at pH 3.0 the content of the minor form could not be measured accurately because of extensive overlap of the peaks of the major and minor forms. The temperature dependence of the ratio between the concentrations of the two observed forms led to the conclusion that there is a dynamic equilibrium between two different conformations of LqhαIT. The ratio of the conformational variants in the R64H sample was identical to that of the unmodified toxin.

The most prominent examples of conformational heterogeneity included the aromatic resonances of both the major (Tyr^5, Tyr^{35}, Tyr^{42}, Trp^{47}, and Tyr^{49}) and minor (Tyr^{14}) hydrophobic clusters as well as Trp^{38}. Surprisingly, the backbone resonances of several residues belonging to the secondary structure elements (Leu^{25} and Lys^{28} in the α-helix and Asp^3, Tyr^5, Trp^{38}, Asn^{45}, Cys^{46}, Trp^{47}, and Cys^{48} in the β-sheet) also had two conformational forms.

Since the two conformations were present in different amounts, the chemical exchange could lead to more substantial line broadening in the minor form than in the major form. It was demonstrated by Wüthrich and co-workers

(Otting et al., 1993) that, provided the natural line width for both conformations is the same, the difference of half-height line widths of the minor and major forms is proportional to the difference in the rate constants of the conformational equilibrium and independent of the natural line width. The peaks of the major and minor conformers of several resonances were fitted to Lorentzian line shapes. The differences in half-height line widths enabled us to estimate that the conversion rate of the major form into the minor one is on the order of $1-5\ s^{-1}$ at 308 K. This value is consistent with the result obtained by Bystrov and co-workers (Pashkov et al., 1988) for a similar scorpion toxin, BeM_9.

Spectral data and structural studies are reported only for the major conformer, since quantitation of NOE cross peaks of the minor one was severely complicated by too low signal-to-noise ratios of its peaks for the majority of the residues. The cross peaks chosen as a reference for calibrating the derived distances did not exhibit any conformational analogs. The cross peaks of the major form were treated as if they arised from all toxin molecules, rather than from approximately 75% of the them. As a result, the distances derived from these cross peaks were 5% longer than those that could have been obtained if the intensities of the cross peaks of the major conformation were normalized. This slight overestimation of the distances should not significantly affect the structure calculation. It should be noted that all the detectable cross peaks of the minor conformer were accompanied by much stronger cross peaks of the major one which corresponded to the same interactions. This observation implies only a minor conformational difference between the two forms of the toxin.

NMR Studies of the R64H Mutant of LqhαIT. In most scorpion α-toxins, position 64 is occupied by histidine, whereas arginine is found at this position in LqhαIT and Lqq4. Mutation of Arg^{64} to histidine increased the toxicity of LqhαIT by 3-fold for both insects and mammals (Gurevitz and Zilberberg, unpublished results), indicating the importance of this residue for biological activity of the toxin. To investigate the implications of this mutation on the conformation of the toxin we determined the 3D structure of the R64H mutant.

It is well-known that proton chemical shifts in the fingerprint region of the spectrum are especially sensitive to conformational changes in proteins. As the NMR experiments with the R64H mutant were conducted at exactly the same experimental conditions as those for the unmodified toxin, the changes in chemical shifts are indicative of local conformational perturbations caused by the mutation.

Detailed comparison of the chemical shifts of LqhαIT and the R64H mutant indicated that changes exceeding 0.02 ppm occurred only for residues sequentially proximal to the mutation site (H^N and H^α of Gly^{61}, Lys^{62}, and Cys^{63}) or those spatially adjacent in the LqhαIT structure (especially Asn^9, Tyr^{10}, and Asn^{11}). The most significant changes were observed for Tyr^{10} (0.11 ppm for H^N, 0.16 ppm for H^α, 0.43 and 1.01 ppm for two β-protons) and the β-protons of Asn^9 (0.07 and 0.21 ppm). Interestingly, slight changes were observed also for the side-chain resonances of Arg^{58}. The side chain of this arginine plays an important role in stabilizing the 5-residue Lys^8-Cys^{12} tight turn. This observation may imply that a slight conformational rearrangement of this turn occurred as a result of the R64H mutation.

Backbone−backbone, backbone−side chain, and side chain−side chain interactions between His^{64} and Tyr^{10} were observed in the NOESY spectra of the R64H mutant. The β-protons of Tyr^{10} experience strong ring-current shifts, presumably resulting from their proximity to the aromatic ring of His^{64}. Weak cross peaks between the side-chain protons of Lys^{62} and His^{64} were observed as well. All these observations and the structures calculated with eight long-range distance constraints for His^{64} show that its aromatic ring is close to both Tyr^{10} and Lys^{62} side chains, forming a surface pattern typical of scorpion toxins (an exposed aromatic ring adjacent to a positively charged side chain).

DISCUSSION

Despite similar backbone conformations, scorpion α-toxins are diverse in binding affinities, displaceability characteristics, and phylogenetic preferences. Thus, determination of the 3D structures of either toxins displaying similar structures but different pharmacology or relatively distant structures but identical pharmacology may be useful in correlating structural domains with functional features. In this respect, LqhαIT, the most insecticidal scorpion α-neurotoxin (Eitan et al., 1990; Gordon et al., 1996), and AaHII, the most potent antimammalian α-toxin (Zlotkin et al., 1978), may be suitable for such study. Furthermore, the remarkable homology between LqhαIT and LqqIII (Kopeyan et al., 1993) varying in only three residues (A20S, E24A, and R64H) but displaying a 4-fold difference in phylogenetic preference (Gordon et al., 1996), provides an attractive opportunity to compare their structures and attempt to correlate pharmacological differences with only minor changes in the sequence and three-dimensional structure.

General Features of the LqhαIT Tertiary Structure. The structure of LqhαIT resembles that of other long-chain scorpion toxins. The protein is compact with a well-defined core consisting of an α-helix, a three stranded anti-parallel β-sheet, several loops connecting the β-strands and an additional long loop at the C-terminus. The helix is attached to the β-sheet by two disulfide bridges.

The major hydrophobic patch includes solvent exposed side chains of Tyr^5, Tyr^{35}, Tyr^{42}, Tyr^{49} and Trp^{47}. The orthogonal alignment of aromatic side chains involved in the hydrophobic patch (so called "herringbone" arrangement), was noted from visual inspection of the structures. The "herringbone" motif is found also in other scorpion toxins and is known to be the lowest energy configuration of solvent-exposed aromatic rings (Burley & Petsko, 1985). The second minor hydrophobic patch on the opposite side of the protein is centered around Tyr^{21} and Tyr^{14}, including also δ-methyls of Leu^{25}.

In addition to two type I β-turns identified previously, a third distorted type I turn is observed. This turn is formed by Thr^{27}, Lys^{28}, Asn^{29} and Gly^{30}, and is hardly distinguishable from the helix. It was postulated to be a type I-like turn on the basis of the ϕ and ψ angles obtained in the calculated structures. The *i* and *i+1* residues of this turn belong to the end of the α-helix.

The C-terminal segment of LqhαIT, comprising residues Pro^{56}-Arg^{64}, adopts an unusually well-defined conformation in comparison to the NMR structures of other scorpion toxins (Darbon et al., 1991; Jablonsky et al., 1995). In addition to the Cys^{12}/Cys^{63} disulfide bridge, this conformation is stabilized by hydrogen bonds with the backbone and side-chain

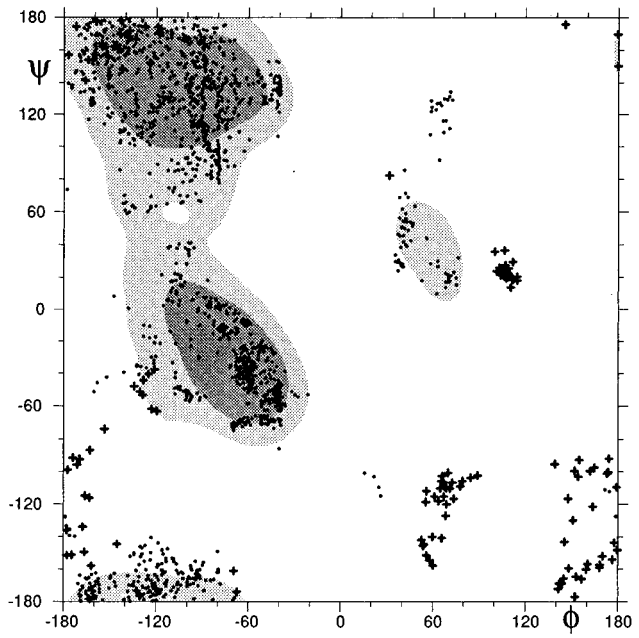

FIGURE 5: Ramachandran plot for the set of 29 LqhαIT structures. The areas of allowed regions are shaded. Glycine residues are represented by plus symbols.

atoms of the 5-residue turn comprising residues Lys[8]-Cys[12]. The side chains of Asn[11] and Arg[58] play a special role in these interactions. The side-chain amide hydrogens of Asn[11] are hydrogen-bonded to the backbone carbonyl of Val[59], whereas H^{ϵ} of Arg[58] is hydrogen-bonded to the backbone carbonyl of Asn[11]. A hydrogen bond between H^{N} of Arg[64] and O of Tyr[10] was also inferred from the NMR data. The aromatic ring of Tyr[10] may interact with the positive charge of the guanidinium group of Arg[64].

Ramachandran plot for the set of 29 LqhαIT structures is shown in Figure 5. The ϕ and ψ angles predominantly occupy allowed regions. Only two non-glycine residues adopt positive ϕ angles in all 29 structures (Ala[50] and Asn[11]). It is well-known that asparagine residues adopt positive ϕ angles in the middle of tight turns more easily than other amino acids (Richardson, 1981). There are also several residues with underdetermined ϕ angle values: Asn[9] tends to adopt ϕ angles from $-60°$ to $+40°$ and is placed in the middle of the 5-residue turn, whereas Ala[39] has positive ϕ angles in a number of the final structures and is positive also in the X-ray structure of AaHII (Fontecilla-Camps et al., 1988).

Conformational Heterogeneity. Conformational heterogeneity was observed previously in 2D NMR studies of a similar scorpion toxin, BeM_9. It was tentatively explained by *cis*−*trans* isomerization of the Lys[8]−Pro[9] bond (Pashkov et al., 1988). This proline is absent in the 5-residue turn of LqhαIT, and no indications of *cis*−*trans* isomerization of any of the three prolines of LqhαIT were obtained from NMR spectra. Another possible explanation proposed was the protonation of one or more carboxyl groups with $pK_a \sim 2$, since at basic pH the spectrum corresponded to only one structural form (Pashkov et al., 1988). It is very unlikely that this could be the case for LqhαIT, which was studied at pH 4.8 and 5.8. The resonances of the second conformational form were observed also in the recent NMR studies of LqqIII, especially near cysteine residues (Landon et al., 1996), implying disulfide bond isomerization. The isomerization of the disulfide bond was thoroughly investigated by NMR for BPTI by Wüthrich and co-workers (Otting et al., 1993). In the case of LqhαIT, however, the residues exhibiting the second conformational form are not necessarily sequentially or spatially localized near cysteines. The differences in chemical shifts between the major and minor conformational forms in LqhαIT are on average much less significant than observed for BPTI. As it is very unlikely that a disulfide bond isomerization would produce long-range structural perturbations comparable to or even stronger than those in its immediate vicinity, these observations suggest that some additional sources of conformational flexibility exist, besides possible isomerization of the disulfides. The latter may not be definitely ruled out, as only three of eight cysteine χ_1 angles were defined in the structure of LqhαIT.

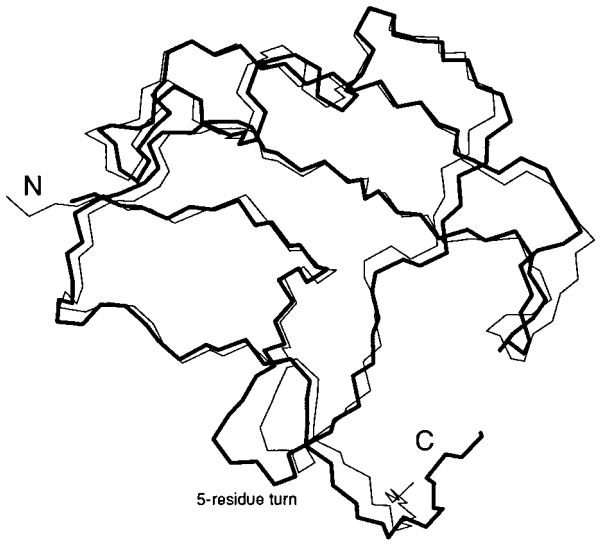

FIGURE 6: Best-fit superposition of the backbone conformations of LqhαIT (thin line) and AaHII (bold line).

Almost all hydrogen atoms of LqhαIT exhibiting the minor conformational form belong to or are located around the major and the minor CHS. The ring rotational motions in the hydrophobic patches of LqhαIT are likely to be concerted because of their spatial proximity and numerous interactions between aromatic protons of different rings. It is not clear whether some concerted rearrangements of the CHS may occur as slowly as to be observable on the chemical shift time scale. The conformational exchange rate in LqhαIT is, however, faster than the amide exchange rate of hydrogen-bonded or buried amide protons. Transient exposure of these protons to the solvent as a result of a conformational rearrangement would considerably enhance their exchange rates. This may be the cause of a faster than usual exchange of the amide protons of several residues of the β-sheet and the α-helix (see Figure 2). Early NMR studies of a highly flexible *Tityus serrulatus* scorpion toxin, for instance, showed that all its amide hydrogens exhibited complete exchange in a matter of minutes at 295 K and pH values from 5.5 to 6.5 (Possani et al., 1981).

Comparison with the AaHII Structure and with the R64H Mutant. The conformation of the polypeptide backbone of LqhαIT toxin is remarkably similar to that of the α-toxin AaHII, whose structure was solved by X-ray crystallography (Fontecilla-Camps et al., 1988). The rmsd for the backbone atoms between the two proteins is only 1.1 Å (see Figure 6). The secondary structure is essentially identical in both

toxins. The location and type of turns in LqhαIT are also very similar to those of AaHII.

The structure of the major conserved hydrophobic surface (CHS) is common to both toxins and the only difference is the substitution of Tyr^{47} in AaHII by tryptophan in LqhαIT. However, in the vicinity of the major CHS, the acid−base pair Lys^{50}−Glu^{32} in AaHII contrasts the neutral amino acids Ala^{50} and Ser^{32} on the surface of LqhαIT. Amino acids at positions 32 and 50 are variable in scorpion toxins but in most cases form an acid−base pair. The structural importance of this difference was indirectly demonstrated by previous mutagenic studies (Zilberberg et al., 1996; see Implications from Mutagenetic Studies below). Interestingly, Lys^{50} in the X-ray structure of AaHII toxin (Fontecilla-Camps et al., 1988) has almost exactly the same positive ϕ angle value as Ala^{50} in the structure of LqhαIT. This generally unfavorable conformation may be at least partially stabilized in both toxins by a hydrogen bond to the carboxylate of Asp^{3}. Asn^{11} was also found to have a positive ϕ angle in AaHII. It was recently shown by *ab initio* quantum mechanical modeling (Herzberg & Moult, 1991) that positive ϕ angles introduce substantial strain in the polypeptidic backbone of proteins and are usually encountered at, or close to, functionally important regions of the molecules.

The 5-residue turn Lys^{8}-Cys^{12} and the last 2−3 residues of the C-terminus, which are spatially closer to the minor CHS, differ considerably between the two toxins. The sequence DDV at the beginning of the 5-residue turn in AaHII is substituted by KNY in LqhαIT. This variation causes changes in the charge of the surface, and different side chain−side chain interactions stabilize the 5-residue turn. The interaction of the aromatic ring of Tyr^{10} with Arg^{64} found in LqhαIT is the most salient difference. Tyr^{10} and Arg^{64} of LqhαIT are rare at these positions in scorpion α-toxins. In AaHII, the side chain of His^{64} points to the opposite direction as compared with Arg^{64} in LqhαIT and is closer to Lys^{62}. The replacement of Arg^{64} by histidine is accompanied by significant changes in the chemical shifts of the β-protons of Tyr^{10}, possibly due to the ring current effect caused by the histidine ring. Another interaction in LqhαIT worth mentioning in this respect is between Lys^{8} and Tyr^{14}. In AaHII, the side chain of Asp^{8} points away from the Tyr^{14} ring.

The side chain of His^{64} in the calculated structure of the R64H mutant is oriented in the opposite direction (almost 180°) relative to that of Arg^{64} in the unmodified toxin. This orientation of His^{64} in the mutant and the mutual arrangement of the side chains of Tyr^{10}, His^{64}, and Lys^{62} is similar to that in AaHII. It may be concluded that the orientation of the side chain of residue 64 depends on specific interactions with the neighboring side chains of the C-terminus and the 5-residue turn. As no other substantial differences were observed between the structures of the unmodified LqhαIT and its mutant, it is likely that the hydrophobicity of the histidine ring is preferable to the polarity of arginine in maintaining the surface pattern necessary for higher levels of toxicity.

Variations in the α-Helix Dictate Pharmacological Differences between LqhαIT and LqqIII. Most recently, a low-resolution NMR structure of a highly homologous α-toxin, LqqIII, was reported (Landon et al., 1996). This toxin differs from LqhαIT in three amino acids at positions 20, 24, and 64 (see Figure 1). The average rmsd of the C^{α} coordinates between AaHII and LqhαIT and between AaHII and LqqIII is 1.1 and 2.6 Å, respectively, indicating that the backbone of LqhαIT is more similar to that of AaHII. It is possible that the structure of LqqIII at higher resolution, when it becomes available, will be more similar to that of LqhαIT. LqhαIT and LqqIII differ also in their antiinsect/antimammalian toxicity ratio in favor of LqhαIT (Gordon et al., 1996). LD_{50} on the cockroach *Blatella germanica* is 3.3-fold lower for LqhαIT and 1.2-fold higher on mice. Analysis of the bioactivity of the R64H mutant enabled us to discriminate among the roles of the residues, which differ in the two toxins. The toxicity of the R64H mutant increased 3-fold against both insects (ED_{50} and IC_{50}) and mammals (LD_{50}) (Gurevitz and Zilberberg, unpublished results), and therefore, in comparison to LqqIII, the R64H mutant is ∼10 times more toxic to insects and ∼2.5 times more toxic to mammals.

The chemical shifts of LqhαIT and LqqIII are very similar. However, since the NMR experiments on LqqIII (Landon et al., 1996) were conducted at a slightly lower pH value (4.2 vs 4.8 for LqhαIT and the R64H mutant), differences do exist, especially in the chemical shifts of some amide protons (H^{N} of Arg^{2}, Cys^{36}, Ala^{50}, Asp^{53}, and Val^{55}). It was noted from comparisons of the HOHAHA spectra of LqhαIT recorded at different pH values that the chemical shifts of backbone and side-chain hydrogens of residues, spatially adjacent to the N-terminus and the 52−55 tight turn (e.g., H^{N} of Arg^{2}, Asp^{53}, and Val^{55}), are especially sensitive to pH. This may be attributed to a lower stability of the dense hydrogen-bonding network of this region of the molecule at lower pH values due to the protonation of charged groups involved in maintaining the tertiary structure. The differences in chemical shifts of the H^{N} protons of Ala^{50} and Cys^{36} between LqqIII and LqhαIT may be due to hydrogen bonds of these amide protons with the carboxyls of Asp^{3} and Asp^{19}, respectively, in both AaHII and LqHαIT.

Significant differences in chemical shifts between LqqIII and LqhαIT were observed also for the H^{N} and H^{β} of Tyr^{10}. These protons are spatially close to the side-chain protons of Arg^{64} in the LqhαIT structure. The chemical shift difference could be attributed to the substitution of Arg^{64} by histidine in the sequence of LqqIII. Indeed, in the HOHAHA spectrum of the R64H mutant of LqhαIT the chemical shifts of Tyr^{10} were identical to those of LqqIII. This identity in chemical shifts suggests that the mutual orientation of Tyr^{10}, Lys^{62}, and His^{64} is similar in LqqIII and the R64H mutant.

As the conformation of His^{64} and its vicinity is very similar in both the R64H mutant and LqqIII, it may be concluded that the replacement of Ala^{20} and Glu^{24} of LqhαIT by Ser and Ala, respectively, in LqqIII accounts for the difference in phylogenetic selectivity between LqhαIT and LqqIII as well as between the R64H mutant and LqqIII. However, it is possible that residues 20 and 24 would not directly interact with the receptor site, as antibodies raised against the α-helical region of AaHII were capable of binding to the toxin when it was bound to the receptor site (El Ayeb et al., 1986). The two differences between LqhαIT and LqqIII in the sequence of the α-helix may possibly generate variations in the metabolic fate and stability upon injection to test animals. The decreased IC_{50} value measured with the R64H mutant of LqhαIT as compared to LqqIII (both bearing a C-terminal histidine) suggests that the structural variations

between LqhαIT and LqqIII affect the binding properties to the receptor site. This finding could be explained by the relative proximity of these residues to the minor hydrophobic patch, provided this patch is involved in the toxic site region.

Implications from Mutagenetic Studies. The study of structure−function relationship of α-scorpion toxins affecting sodium channels has been limited till recently to a number of chemical modifications (Darbon et al., 1983; Kharrat et al., 1989; El Ayeb et al., 1986). The recent success in efficient production of a functional recombinant LqhαIT (Zilberberg et al., 1996) has paved the way for site-directed mutagenesis studies, aimed at a better understanding of the structural basis for the animal group specificity of scorpion α-toxins. The structural differences between LqhαIT and AaHII may serve as a basis for mutational analysis to evaluate the role of the 5-residue turn, the C-terminal region, their mutual disposition, and other possible intramolecular interactions unique to LqhαIT.

The recent genetic modification of three residues adjacent to the main hydrophobic cluster (Y49I, A50K, and N54K) had a negligible effect on the toxicity to fly larvae and on the binding affinity to an insect receptor site and decreased the antimammalian toxicity 6.4-fold (Zilberberg et al., 1996). This triple mutation generated a C-terminal half similar to that of Lqq4 (Kopeyan et al., 1985). The unexpected result of such a modification may be tentatively explained by the existence of the acid−base pair Lys^{51}−Glu^{33} in Lqq4 (a shift of one residue in Lqq4 is due to the presence of an additional glycine at the N-terminus). The same acid−base pair is present in AaHII and almost in all other scorpion α-toxins. The lack of this salt bridge in both LqhαIT and LqqIII suggests that it may play a role in antimammalian activity. The mutation A50K alone (without compensating the positive charge by a concomitant S32E mutation) may be detrimental for antimammalian toxicity and may modulate the phylogenetic preference if these two residues are involved in binding. Hence, it would be interesting to investigate the result of a quadruple mutation: Y49I, A50K, N54K, and S32E. The observation that residue 50 in both LqhαIT and AaHII adopts an unusual positive ϕ angle gives an additional indication that this residue and its vicinity play an important functional role in the two toxins.

Preliminary studies of the mutations introduced at the 5-residue turn and the C-terminus including the R64H mutation suggest that this region of LqhαIT may be involved in recognition of the receptor site. The amino acid substitutions at these regions produced critical effects on biological activity (Gurevitz and Zilberberg, unpublished results). These results are in concert with the conclusions of the present work regarding structural differences between LqhαIT and AaHII.

ACKNOWLEDGMENT

We are highly indebted to Professor M. Levitt for fruitful discussions and invaluable help in structure calculations. We also thank Mr. Y. Hayek for help in purification of the toxins. Useful comments and suggestions of Dr. T. Scherf, Dr. A. Zvi, and Mr. O. Froy are gratefully acknowledged. The use of the MOLMOL program in structural analysis was made possible due to the kind cooperation of Dr. R. Koradi.

SUPPORTING INFORMATION AVAILABLE

One table containing the chemical shifts of the unmodified LqhαIT toxin at 308 K and pH 4.8 (2 pages). Ordering information is given on any current masthead page.

REFERENCES

Basus, V. L. (1989) *Methods Enzymol. 177*, 132.
Beneski, D. A., & Catterall, W. A. (1980) *Proc. Natl. Acad. Sci. U.S.A. 77*, 639−643.
Braun, W., Bösch, C., Brown, L. R., Go, N., & Wüthrich, K. (1981) *Biochim. Biophys. Acta 667*, 377−396.
Brünger, A. T. (1992) *XPLOR 3.1 Manual*, Yale University Press, New Haven, CT.
Brünger, A. T., Clore, G. M., Gronenborn, A. M., & Karplus, M. (1986) *Proc. Natl. Acad. Sci. U.S.A. 83*, 3801−3805.
Burley, S. K., & Petsko, G. A. (1985) *Science 240*, 23−28.
Catterall, W. A. (1977) *J. Biol. Chem. 252*, 8660−8668.
Clore, M., & Gronenborn, A. (1989) *Crit. Rev. Biochem. Mol. Biol. 5*, 479−564.
Darbon, H., Jover, E., Couraud, F., & Rochat, H. (1983) *Int. J. Pept. Protein Res. 22*, 179−186.
Darbon, H., Weber, C., & Braun, W. (1991) *Biochemistry 30*, 1836−1845.
Davis, D. G., & Bax, A. (1985) *J. Am. Chem. Soc. 107*, 2820−2821.
Driscoll, P. C., Clore, G. M., Beress, L., & Gronenborn, A. M. (1989) *Biochemistry 28*, 2178.
Dufton, M. S., & Rochat, H. (1984) *J. Mol. Evol. 20*, 120−127.
Eitan, M., Fowler, E., Herrmann, R., Duval, A., Pelhate, M., & Zlotkin, E. (1990) *Biochemistry 29*, 5941−5947.
El Ayeb, M., Bahraoui, E. M., Granier, C., & Rochat, H. (1986) *Biochemistry 25*, 6671−6678.
Fontecilla-Camps, J. C. (1989) *J. Mol. Evol. 29*, 63−67.
Fontecilla-Camps, J. C., Almassy, R. J., Suddath, F. L., & Bugg, C. E. (1982) *Toxicon 20*, 1−7.
Fontecilla-Camps, J. C., Habersetzer-Rochat, C., & Rochat, H. (1988) *Proc. Natl. Acad. Sci. U.S.A. 85*, 7443−7447.
Gordon, D., & Zlotkin, E. (1993) *FEBS Lett. 315*, 125−128.
Gordon, D., Martin-Euclair, M.-F., Cestele, S., Kopeyan, C., Carlier, E., Ben Khalifa, R., Pelhate, M., & Rochat, H. (1996) *J. Biol. Chem. 271*, 8034−8045.
Herzberg, O., & Moult, J. (1991) *Proteins: Struct., Funct., Genet. 11*, 223−229.
Jablonsky, M., Watt, D., & Krishna, R. (1995) *J. Mol. Biol. 248*, 449−458.
Kharrat, R., Darbon, H., Rochat, H., & Granier, C. (1989) *Eur. J. Biochem. 181*, 381−390.
Kopeyan, L., Martinez, G., & Rochat, H. (1985) *FEBS Lett. 181*, 211−217.
Kopeyan, C., Mansuelle, P., Martin-Eauclaire, M. F., Rochat, H., & Miranda, F. (1993) *Nat. Toxins 1*, 308−312.
Kumar, A., Ernst, R. R., & Wüthrich, K. (1980) *Biochem. Biophys. Res. Commun. 95*, 1−6.
Landon, C., Cornet, B., Bonmatin, J.-M., Kopeyan, C., Rochat, H., Vovelle, F., & Ptak, M. (1996) *Eur. J. Biochem. 236*, 395−404.
Lebreton, F., Delepierre, M., Ramírez, A. N., Balderas, C., & Possani, L. D. (1994) *Biochemistry 33*, 11135−11149.
Macura, S., & Ernst, R. R. (1981) *Mol. Phys. 41*, 95−117.
Marion, D., & Wüthrich, K. (1983) *Biochem. Biophys. Res. Commun. 113*, 967−974.
Neidig, K.-P., Geyer, M., Gorler, A., Antz, C., Saffrich, R., Beneicke, W., & Kalbitzer, H. R. (1995) *J. Biomol. NMR 6*, 255−270.
Nilges, M. (1993) *Proteins: Struct., Funct., Genet. 17*, 297−309.
Nilges, M., Clore, M., & Gronenborn, A. (1988) *FEBS Lett. 229*, 317−324.
Otting, G., Liepinsh, E., & Wüthrich, K. (1993) *Biochemistry 32*, 3571−3582.
Pashkov, V., Maiorov, V., Bystrov, V., Hoang, A., Volkova, M., & Grishin, E. (1988) *Biophys. Chem. 31*, 121−131.
Piantini, U., Sørensen, O., & Ernst, R. R. (1982) *J. Am. Chem. Soc. 104*, 6800−6801.

Piotto, M., Saudek., V., & Sklenar, V. (1992) *J. Biomol. NMR 2*, 661−669.
Possani, L., Steinmetz, W. E., Dent, M. A. R., Alagón, A. C., & Wüthrich, K. (1981) *Biochim. Biophys. Acta 669*, 183−192.
Richardson, J. S. (1981) *Adv. Protein Chem. 34*, 167−339.
Rochat, H., Bernard, P., & Couraud, F. (1979) in *Advances in Cytopharmacology* (Ceccarelli, B., & Clementi, F., Eds.) Vol. 3, pp 325−334, Raven Press, New York.
Shaka, A. J., Keeler, J., Frenkiel, T. A., & Freeman, R. (1983) *J. Magn. Reson. 52*, 335−343.
Wagner, G., Braun, W., Havel, T. F., Schaumann, T., Go, N., & Wüthrich, K. (1987) *J. Mol. Biol. 196*, 611.
Wishart, D. S., Sykes, B. D., & Richards, F. M. (1991) *J. Mol. Biol. 222*, 311−333.
Wishart, D. S., Sykes, B. D., & Richards, F. M. (1992) *Biochemistry 31*, 1647−1651.
Wüthrich, K. (1986) *NMR of Proteins and Nucleic Acids*, Wiley Publishers, New York.
Wüthrich, K. (1989) *Acc. Chem. Res. 22*, 36−44.
Wüthrich, K., Billeter, M., & Braun, W. (1983) *J. Mol. Biol. 169*, 949−961.
Zhao, B., Carson, M., Ealick, S., & Bugg, C. (1992) *J. Mol. Biol. 227*, 239−252.
Zilberberg, N., Gordon, D., Zlotkin, E., Pelhate, M., Norris, T., Adams, M. E., & Gurevitz, M. (1996) *Biochemistry 35*, 10215−10222.
Zlotkin, E., Miranda, F., & Rochat, H. (1978) in *Arthropod Venoms* (Bettini, S., Ed.) pp 317−369, Springer, Berlin and Heidelberg, Germany.
Zuiderweg, E. R. P., Böelens, R., & Kaptein, R. (1985) *Biopolymers 24*, 601.

BI961497L